Longitudinal trajectories of resilient psychosocial functioning link to ongoing cortical myelination and functional reorganization during adolescence

Meike D. Hettwer (1-4), Lena Dorfschmidt (6-9), Lara Puhlmann (4,10), Linda M. Jacob (4), Casey Paquola (3), Richard A. I. Bethlehem (11), NSPN Consortium (†), Edward T. Bullmore (6), Simon B. Eickhoff (1-3), Sofie L. Valk (1-4)**

1) Institute of Systems Neuroscience, Medical Faculty and University Hospital Düsseldorf, Heinrich Heine University Düsseldorf, Düsseldorf, Germany
2) Max Planck School of Cognition, Max Planck Institute for Human Cognitive and Brain Sciences, Leipzig, Germany
3) Institute of Neuroscience and Medicine, Brain & Behavior (INM-7), Research Centre Jülich, Jülich, Germany
4) Max Planck Institute for Human Cognitive and Brain Sciences, Leipzig, Germany
6) Department of Psychiatry, University of Cambridge, Cambridge, UK
7) Lifespan Brain Institute, The Children's Hospital of Philadelphia and Penn Medicine, Philadelphia PA 19139, USA
8) Department of Biostatistics, Epidemiology and Informatics, University of Pennsylvania, Philadelphia, PA 19104, USA
9) Department of Child and Adolescent Psychiatry and Behavioral Sciences, Children's Hospital of Philadelphia, Philadelphia PA 19139, USA
10) Leibniz Institute for Resilience Research, Mainz, Germany
11) Department of Psychology, University of Cambridge, Cambridge, UK
†) A complete list of the NSPN Consortium can be found in the Supplementary Materials.

* Correspondence to Meike D. Hettwer (m.hettwer@fz-juelich.de) and Sofie L. Valk (valk@cbs.mpg.de)

Abstract

Adolescence is a period of dynamic brain remodeling and susceptibility to psychiatric risk factors, mediated by the protracted consolidation of association cortices. Here, we investigated whether intra-individual trajectories of psychosocial functioning relative to environmental stressor exposure - including adverse life events, dysfunctional family settings, and socio-economic status - are tied to myeloarchitectural maturation and down-stream effects on intrinsic function. To this end, we employed longitudinal myelin-sensitive Magnetic Transfer (MT) and resting-state imaging in the NSPN cohort (aged 14-26y). Developing towards more resilient psychosocial functioning was linked to increasing myelination in the anterolateral prefrontal cortex, which exhibited stabilized functional connectivity. Studying depth-specific intracortical MT profiles and the cortex-wide synchronization of myeloarchitectural maturation, we further observed wide-spread myeloarchitectural re-configuration of association cortices paralleled by attenuated functional reorganization with increasingly resilient outcomes. Together, trajectories of resilient/susceptible psychosocial functioning showed considerable intra-individual change reflected in multi-modal cortical refinement processes at the local and system-level.

Introduction

Adolescence is a period of marked brain remodeling mediating biological and psychosocial maturation, but also heightened susceptibility to environmental adversity that can impact developmental trajectories [1,2]. Studying longitudinal trajectories in the presence of adversity exposure [3] and psychiatric symptoms [2,4,5] has thus been fundamental to advancing our understanding of inter- and intra-individual differences in psychiatric susceptibility. At the same time, there is a growing emphasis on recognizing that many individuals retain mental well-being despite adversity, i.e., show resilient adaptation [6–8]. To comprehend bio-behavioral adaptation to a constantly changing environment, it has been vital to integrate neurodevelopmental assessments, complementary to inter-personal and physiological factors. Converging evidence from cross-sectional studies has highlighted brain regions involved in emotion regulation and stress reactivity in association with adolescent susceptibility or resilience to environmental adversity. Specifically, resilient adaptation has been linked to greater prefrontal and hippocampal volumes, increased prefrontal regulation of amygdala activity, attenuated amygdala responses to adverse stimuli, and increased structural connectivity in the corpus callosum [9,10]. In the past decade, however, psychosocial conceptualizations have increasingly highlighted the dynamic nature of resilience [7,9,11–14]. Correspondingly, the ability to adapt to environmental adversity may show considerable intra-individual changes tied to plastic neurodevelopment. Yet, longitudinal studies probing this notion, especially during periods of heightened susceptibility to psychopathology, remain scarce [1,9,15].

Throughout adolescent brain development, intra- and inter-regional connections are continuously myelinated to enhance circuit efficiency [16,17]. While myelination restricts structural plasticity by consolidating established connections, it has also been found to continuously modulate network dynamics to adapt to ever changing environmental circumstances [17,18]. Notably, rates of myelin maturation are heterochronous across the cortex. Strongly interconnected association cortices show particularly protracted myelination [19–21], which likely reflects later refinement of functional networks associated with abstract cognitive functions, such as cognitive control, but also renders them more susceptible to environmental impact and psychopathological alterations [19–21]. Thus, the dual role of myelin both in consolidation and dynamic functional adaptation makes the study of ongoing adolescent myelination a compelling focus in the framework of adaptive psychosocial trajectories.

Recent advances in *in vivo* mapping of cortical myelin have improved our understanding of mesoscale maturation. One promising imaging contrast is magnetic transfer saturation (MT) [22], which is dominated by myelin-related molecules in the brain, as has been verified by several histological validation studies [23–25]. Moreover, it has been demonstrated to be sensitive to both developmental processes [5,20,26] and pathological alterations in myelin content [27]. Aiming for nuanced insights into age-related changes in intracortical myeloarchitecture, several studies have sampled myelin-proxies across intra-cortical depths perpendicular to the cortical mantle, commonly referred to as “cortical profiling” [5,20]. Such depth-dependent profiling enables the analysis of synchronized, large-scale patterns of cortical myeloarchitectural development by quantifying changes in inter-regional similarities (microstructural profile covariance; MPC). Previous work indicates that microstructural similarity predicts cortico-cortical connectivity [28,29]. Thus, studying changes in MPC with age yields valuable insights into system-level microstructural integration and differentiation, and its potential link to functional reorganization [30,30,31]. Association areas, in particular, represent a nexus of mixed intra-cortical profiles [32,33] that show marked and partly synchronized refinement well into early adulthood [20]. This organization may be central in supporting the maturation of intrinsic functional organization of the default and frontal parietal networks, mediating abstract cognitive operations such as cognitive control or emotional flexibility [34,35]. Together, leveraging multi-modal, global approaches is imperative to unravel the complex role of

system-wide cortical refinement for mental health and aligns with the broader understanding of maturational and psychopathological cortical alterations occurring in a network-like fashion [36,37].

In the current study, we investigated myeloarchitectural maturation associated with trajectories of psychosocial functioning relative to differences in environmental adversity exposure. Psychosocial environmental stressors included dysfunctional family settings, significant adverse life events, and low socio-economic status, at two consecutive time points in adolescents aged 14-26y. For each timepoint, we quantified a continuous stressor resilience score (SRS) as an adjusted measure of psychosocial functioning. SRS reflect deviations from psychosocial distress levels predicted by the stressor load an individual faced [7,38]. That is, lower-than-expected distress reflected resilient adaptation, whereas higher-than-expected distress reflected higher susceptibility to environmental stressors [38]. We then investigated associations between intra-individual changes in SRS and brain maturation, specifically focusing on the role of ongoing myelination [16,19] and the impact on intrinsic function. We observed that longitudinal development towards more susceptible or resilient outcomes were associated with differential rates of prefrontal myelination, prefrontal functional network maturation, and cortex-wide myeloarchitectural re-organization of association cortices. Expanding on cross-sectional studies suggesting increased susceptibility of association cortices to environmental impact [19–21], we thus conclude that adolescent maturational trajectories of brain areas typically implicated in psychopathology are tied to dynamic intra-individual changes in psychosocial functioning relative to adversity.

Results

Stressor resilience scores (Figure 1)

We quantified continuous stressor resilience scores (SRS) by predicting psychosocial distress from measures of environmental adversity (**Figure 1A**). Briefly, we derived a latent factor (**Supplementary Table S1**; $chi^2 = 34293$, $p < 0.001$), reflecting levels of psychosocial distress across domains of anxiety, depression, antisocial and compulsive-obsessive behavior, self-esteem, psychotic-like experiences, and mental well-being (similar to [38,39]). In a supervised random forest prediction, we then predicted psychosocial distress scores from adverse life events, childhood trauma, parenting style, family situation, and socioeconomic status ($R^2 = 0.21$, MAE = 15.15, correlation between true and predicted distress scores: $r = 0.46$). The inverted deviations between true and predicted distress, i.e., the model residuals, were extracted to quantify SRS. SRS thus reflect a spectrum ranging from susceptible to resilient outcomes, i.e., the extent to which an individual shows higher or lower distress levels than expected given their stressor exposure (for similar approaches, see: [38,40–43]). For parsimony, we will refer to this spectrum as stressor resilience scores / resilient psychosocial functioning, which shall include the susceptible (negative) end of the spectrum. See **Supplementary Table S2** for links to demographics.

Different sub-samples were included across analyses in this study (**Figure 1A;** see **Supplementary Methods** for details): The computation of distress score loadings ($n = 1533$) and the prediction from adversity measures ($n = 712$; sub-sample with additional NSPN U-change questionnaires) were conducted in independent samples to avoid leakage effects. Extracted from the $n = 712$ sub-sample, we studied fundamental patterns of MT maturation in $n = 199$, subsequently referred to as the full imaging sample, for whom longitudinal imaging data was available. We then linked longitudinal imaging patterns to change in SRS in $n = 141$ individuals who additionally completed all included questionnaires at repeated timepoints.

Fundamental patterns of MT maturation in the full imaging sample

We started our investigations by evaluating fundamental myeloarchitectural patterns in the full imaging sample (n = 199; 18.83 ± 2.84y; 96 female), to better understand potentially altered trajectories of resilient psychosocial functioning in the next step. We visualized the group-averaged regional MT change between first and last imaging sessions (ΔMT) and observed a wide-spread intra-individual increase in MT (**Figure 1B;** 1.26 ± 0.34y apart). ΔMT was highest towards frontal and temporal poles with strongest inter-individual variability (std) in the ventral prefrontal cortex. Systematic sampling of myelin-sensitive MT intensities along 10 equivolumetric surfaces perpendicular to the cortical mantle further revealed generally highest mean and inter-individual variability in ΔMT in mid-to-deeper layers.

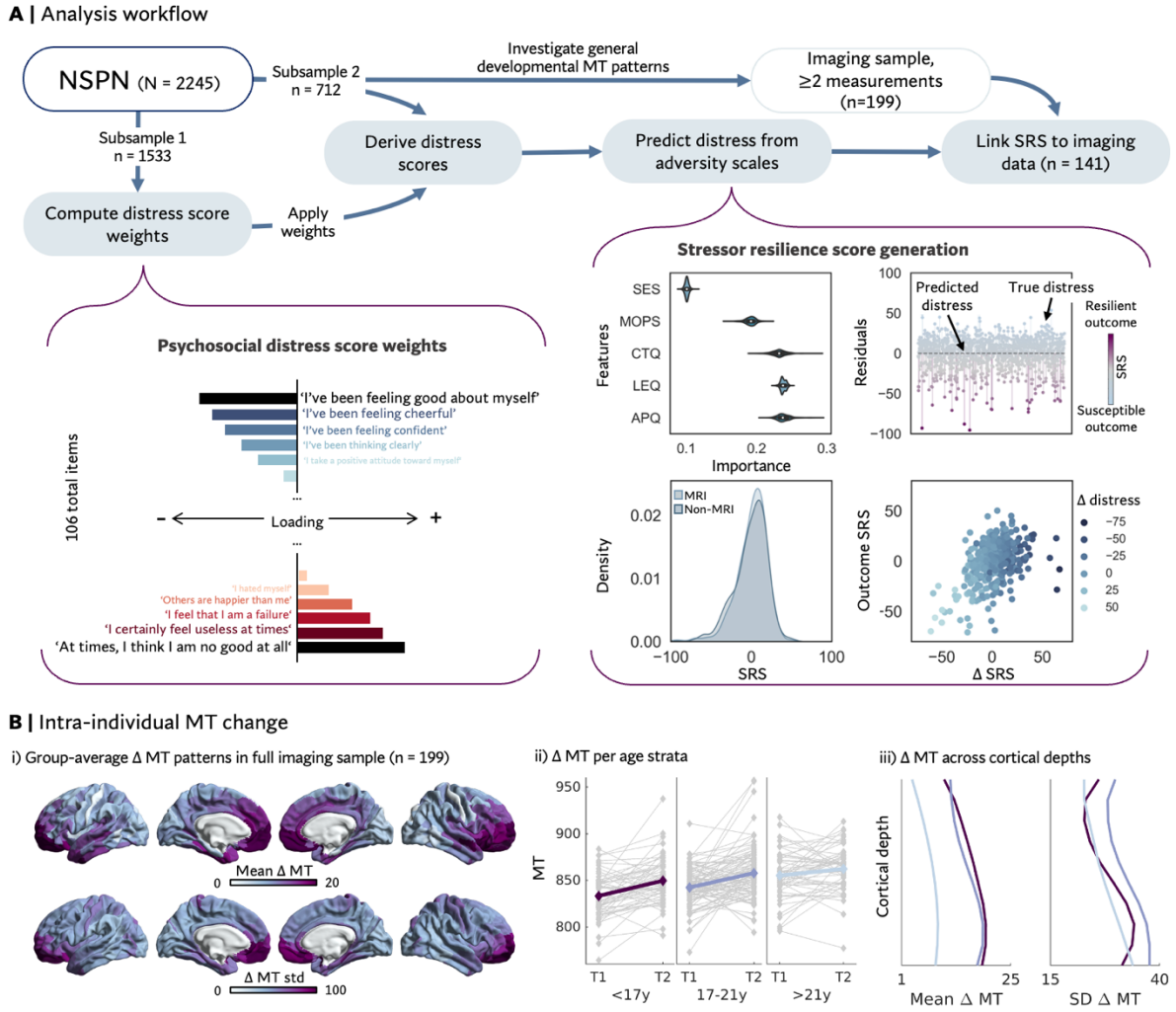

Figure 1. ***Behavioral analysis workflow and group-average longitudinal change in myelin-sensitive Magnetic Transfer (MT).*** **A)** Stressor resilience scores (SRS) were computed for each subject at each available time point by predicting psychosocial distress (left) from adversity assessments (Alabama parenting questionnaire (APQ), Life events questionnaire (LEQ), Childhood trauma questionnaire (CTQ), Measure of Parenting style (MOPS), and socio-economic status (SES)). The SRS was defined as the difference between observed and predicted distress, i.e., showing higher (i.e., more susceptible) or lower (i.e., more resilient) than expected psychosocial distress. **B)** i) Mean and SD of intra-individual change in myelin-sensitive Magnetic Transfer (ΔMT) in the full imaging sample (n=199). ii) ΔMT averaged across the cortex and visualized for three age strata. iii) Mean and SD of ΔMT across 10 intracortical depths and across the cortex. Line colors for ii) and ii) reflect age strata defined in the Middle panel.

Intra-individual trajectories of resilient psychosocial functioning and myelin-sensitive MT (Figure 2)

Once longitudinal MT patterns and stressor resilience scores had been determined, we aimed to elucidate the association between ongoing myelination in adolescence and change in SRS in $n = 141$ individuals for whom both repeated imaging and behavioral assessments were available. We observed a positive association between developing towards more resilient functioning (i.e., an intra-individual increase in SRS) and ΔMT in the predominantly left-lateralized anterolateral prefrontal cortex (PFC; $t_{max} = 4.47$; $p_{10,000\ permutations\ \&\ FDR} < 0.05$; **Figure 2A**). This effect was robust to several analytical choices and sub-sampling (see **Supplementary Figure S2**). Given that rates of myelination are not homogeneous across cortical depths (see **Figure 1B iii**), we further tested for intracortical differentiability of the observed effect within the prefrontal cluster. The positive association between ΔSRS and ΔMT was homogeneous across 10 intra-cortical sampling depths (**Figure 2A ii**). We next assessed whether ΔSRS effects are systematically found in specific cytoarchitectonic cortical types along a histologically defined hierarchy of microstructural complexity [28]. We observed that parcels showing a significant ΔSRS effect were located in Eulaminate cortex II & III (**Figure 2B),** which hold regions with comparatively high cytoarchitectonic complexity and layer differentiation. Overall, the cortical topology of the unthresholded *t*-map followed a general posterior-to-anterior patterning, aligning with a cortex-wide axis of MT development (**Supplementary Figure S3**)

Probing whether observed longitudinal effects may link to cross-sectional differences at baseline, we observed no cross-sectional association between SRS and MT. One medial frontal gyrus parcel showed lower baseline MT in individuals who had a lower SRS at baseline compared to follow-up (see **Supplementary Figure S4**).

Intra-individual change in intrinsic functional connectivity of the anterolateral prefrontal cortex

Having established a positive link between myelin-sensitive MT increase and intra-individual change in SRS, we next investigated concordant changes in the prefrontal cluster's intrinsic functional connectivity (**Figure 2C**). To this end, we defined the identified prefrontal parcels exhibiting a significant effect in MT analyses as a seed and assessed both global (i.e., degree centrality) and network-level effects of ΔSRS on change in intrinsic functional connectivity (ΔFC). Globally, we observed more maintained levels of cortex-wide functional connectivity with increasingly resilient outcomes, whereas increasingly susceptible outcomes were associated with a segregation ($t(134) = 2.44$; $p = 0.02$). Studying the cortex-wide pattern of associations between ΔSRS and prefrontal ΔFC revealed that effects were concentrated in regions of the default mode, frontoparietal and ventral attention networks ($p_{10,000\ permutations\ \&\ FDR} < 0.05$; **Figure 2C & D**) and were driven by sub-regions of the PFC cluster which are part of the default mode network (see **Supplementary Figure S5**).

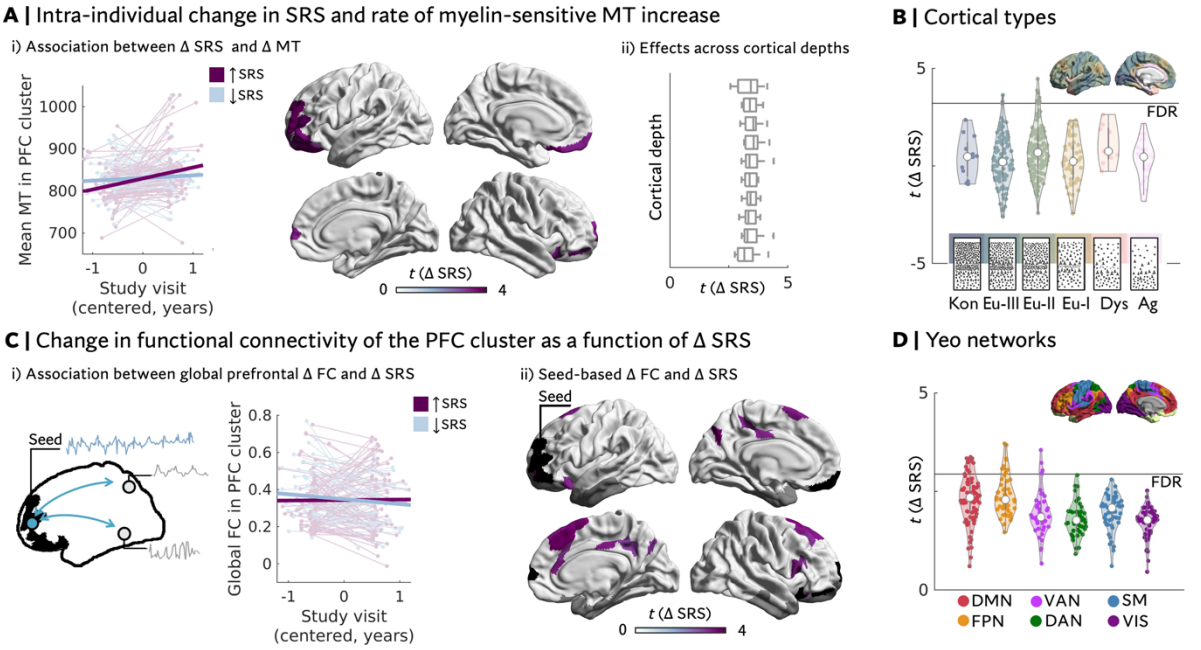

Figure 2. ***Development of resilient psychosocial functioning is associated with trajectories of anterolateral prefrontal myelin-sensitive Magnetic Transfer (MT) and functional connectivity***. **A)** i) Adolescents who showed increasingly resilient responses to psychosocial stressors with age (i.e., increasing stressor resilience scores (SRS)) showed a higher rate of (primarily left) prefrontal myelin-sensitive MT ($p < 0.05$, FDR corrected, 10,000 permutations). ii) This effect was on average homogeneous across cortical depth (box plots for each intra-cortical surface include t-values derived for significant regions depicted in i)), and located in Eulaminate Cortex II and III (**B**). Defining the cluster identified in **A)** as a seed **(C)**, we further observed that functional connectivity (FC) was more globally maintained (i) with increasing SRS. Across the cortex (ii), this effect was most prominent in default mode (DMN) and frontoparietal (FPN) networks **(D)**. Grey masks in functional data reflect parcels that were excluded due to low signal-to-noise ratios. Note that line plots in Ai) and Ci) are colored with respect to increasing vs. decreasing SRS for visualization, but analyses were performed on continuous SRS scores. Kon = Konicortex, Eu-I-III = Eulaminate I-III, Dys = Dysgranular, Ag = Agranular; VAN = Ventral attention network, DAN = Dorsal attention network, SM = Sensorimotor, VIS = Visual.

System-level cortical maturation (Figure 3)

So far, our analyses suggest a role of local prefrontal myeloarchitectural and inter-regional functional network maturation in developmental trajectories of susceptible/resilient psychosocial functioning. This suggests local microstructural alterations may also reflect system-level cortical refinement. Thus, we next aimed to study system-level myeloarchitectural and parallel functional re-organization underlying SRS changes. To this end, we derived a microstructural profile covariance (MPC) matrix, reflecting inter-regional similarities of myeloarchitectural profiles which were derived from probing MT intensities in ten equally spaced intra-cortical depth compartments (**Figure 3A**). Next, we computed a maturational index (MI_{MPC}; **Figure 3B**) which captures age-related change of all MPC edges of a node as a function of respective baseline patterns (estimated for age 14 [44]). The MI_{MPC} revealed a topologically heterogeneous pattern of re-organization ($p<0.05$, FDR). Overall, we observed a U-shaped association between the MI_{MPC} and a previously established [20] principal axis of age-related change (**Figure 3C-E**), which captures a differentiation of idiotypic sensory vs. paralimbic/temporal maturational patterns. Regions at the apices of the axis exhibited a positive MI_{MPC}, i.e., a positive correlation between baseline and change patterns. A positive MI_{MPC} reflects an integration of regions that showed higher myeloarchitectural similarity at baseline and/or a differentiation of regions that were already dissimilar at baseline. This strengthening of existing patterns has been termed 'conservative' development [44].

Conversely, towards the middle of the axis, we observed negative MI_{MPC}, indicating a re-organization of MPC embedding. Here, regions that were more dissimilar at baseline became more integrated with each other and/or regions with higher myeloarchitectural similarity became more differentiated. This is termed 'disruptive' re-organization (which does not imply pathological disruption, but a disruption of baseline patterns during development).

Given the intricate link between system-level structural and functional development [34,45], we studied the convergence of myeloarchitectural and functional maturational modes. The MI based on functional connectivity (MI_{FC}) is characterized by a clear differentiation of 'conservative' development in unimodal regions and 'disruptive' re-organization in association areas (**Figure 3F;** [44]). We found parallel conservative development as well as MPC-reorganization co-occurring with conservative FC development in regions involved in sensory- and attention-related processes (visual, sensorimotor, and ventral attention network). Regions of the default mode and frontoparietal networks showed both cross-modal re-organization and structure-function divergence, in which MPC showed conservative but FC disruptive developmental patterns (**Figure 3G**). Together, this shows that microstructural and intrinsic functional organization show both convergent and divergent maturational patterning at the system-level.

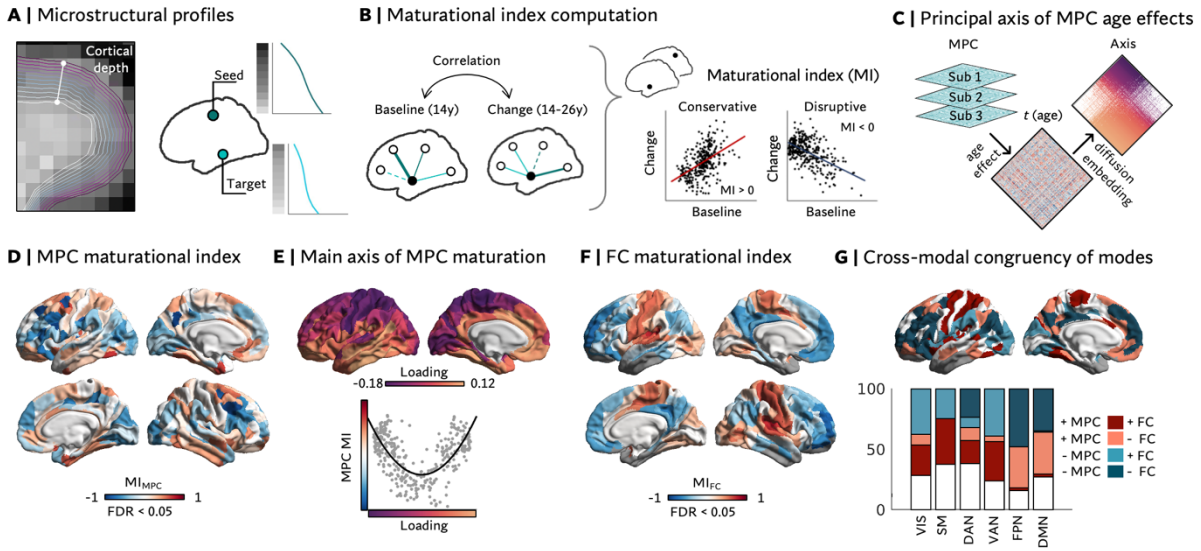

Figure 3. ***Systems-level cortical maturation in the full imaging sample (n = 199), capturing multi-modal re-organization in association cortices.*** **A-C)** depict analytical approaches. **A)** MT intensities were sampled along 10 equi-volumetric surfaces between the gray matter /pial and gray matter /white matter boundaries to derive microstructural profiles and a microstructural profile covariance (MPC) network. **B)** The maturational index captures correlations between baseline (i.e., a pattern predicted for age 14 by a mixed effects general linear model) and change patterns (i.e., the age effect estimated by that model) in a region's network. **C)** A low-dimensional axis of MPC age effects was derived by applying diffusion map embedding to order regions according to their similarity in synchronized microstructural differentiation with age. **D-G)** depict derived maturational patterns. **D)** Maturational index (MI) of MPC (MI_{MPC}; pFDR < 0.05), showing conservative development in ventral temporal and dorsal regions, and disruptive re-organization in heteromodal fronto-parietal cortex. **E)** Relationship between the MI_{MPC} and the principal axis of MPC maturation. The non-linear relationship indicates that conservatively developing ventral and dorsal regions follow maximally different developmental patterns. **F)** MI of functional connectivity (MI_{FC}; pFDR < 0.05), showing conservative development in sensori-motor cortex and disruptive re-organization in heteromodal association cortex. **G)** Maturational categories: Overlaps between MI_{MPC} and MI_{FC} per Yeo network. + = conservative, - = disruptive. VIS = Visual, SM = Sensorimotor, DAN = Dorsal attention network, VAN = Ventral attention network, FPN = Frontoparietal network, DMN: Default mode network. Grey masks in functional data reflect parcels that were excluded due to low signal-to-noise ratios.

System-level maturation and intra-individual change in resilient psychosocial functioning (Figure 4)

Last, we investigated whether trajectories of resilient psychosocial functioning are associated with different degrees of system-level re-organization between the ages of 14 to 26y. As both the MI and the main axis of age-related MPC change are derived from group-level statistics, it was required to form groups for these analyses by dichotomizing trajectories reflecting increasingly resilient (+ΔSRS) vs. increasingly susceptible (-ΔSRS) outcomes. We observed significant group differences between +ΔSRS and -ΔSRS individuals in the MI_{MPC} in 43 predominantly heteromodal regions (**Figure 4A;** $p < 0.05$ FDR & 10,000 permutations). 93% of these regions showed a negative shift in MI_{MPC} in individuals developing towards more resilient outcomes, reflecting mostly less conservative development (58%; **Figure 4B**; **Supplementary Table S3**), but also more disruptive re-organization (19%). Another 16% of these reflected regions that generally showed no significant association between baseline and age-related change patterns in the full imaging sample, that is, in regions that followed neither conservative nor disruptive developmental patterns. Observations were robust to alternative modeling approaches (**Supplementary Figure S6**).

Contextualizing these findings with existing atlases of cortical types [28] and intrinsic functional networks [46] revealed that significant regions were concentrated in Eulaminate-II (35%) and -III (40%) cortex, defined anatomically, and the default mode network (DMN; 37%), defined functionally (**Figure 4B**). In a complementary approach, we investigated MPC trajectories along a low-dimensional cortical axis. We observed a more distinct bimodal distribution of loadings along the principal axis in the group of individuals who developed towards higher susceptibility. That is, regions were situated towards the differentiated apices rather than the middle of the axis, reflecting increasing microstructural similarity with the axis' anchors. Conversely, the axis was slightly compressed in the group of individuals who developed towards more resilient outcomes. Here, more parcels loaded on the middle of the axis reflecting less synchronization with anchor profiles (**Figure 4C**).

Throughout this study, functional connectivity data was used to contextualize myeloarchitectural results. Considering the topology of cross-modal congruency of MIs (**Figure 3G**), we observed that group differences in MI_{MPC} were largely located in regions where MPC and FC did not follow convergent MI patterns (see **Figure 4B**). That is, group differences were most frequently located in regions exhibiting conservative MPC but decoupled, disruptive FC development (35%). The MI_{FC} itself showed subtle group differences in 8 confined, primarily prefrontal regions (**Supplementary Figure S7**). 5 of these regions exhibited less disruptive, 3 exhibited less conservative development in the group of individuals who developed to become more resilient with age.

Together, this suggests that both myeloarchitecture and functional connectivity show marked maturational reorganization tied to resilient/susceptible trajectories of psychosocial functioning, establishing the brain as a key feature of adaptive development.

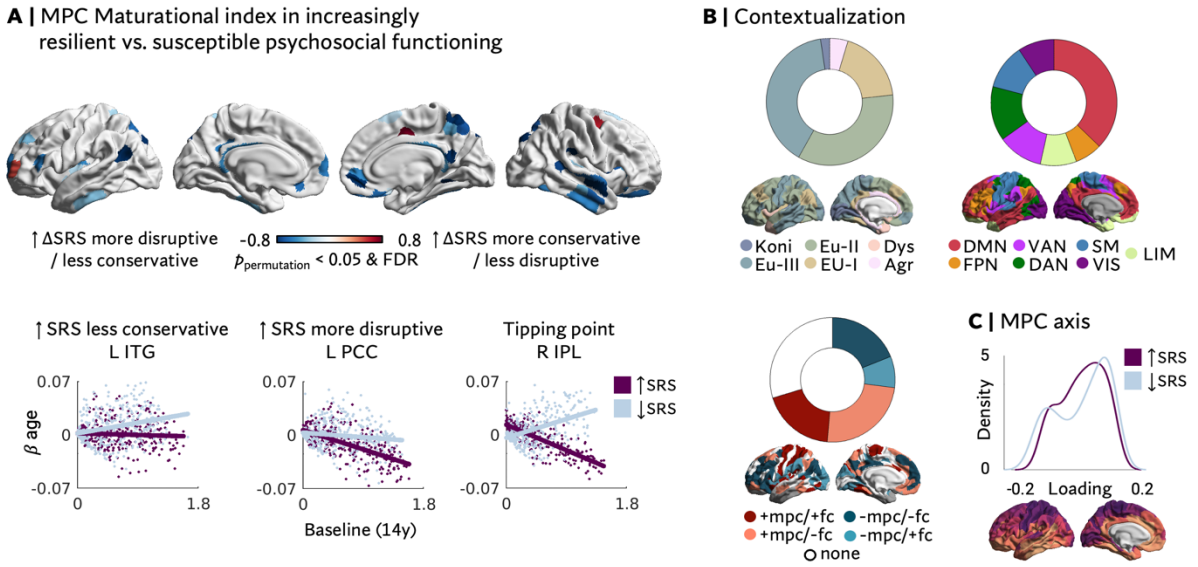

Figure 4. ***More disruptive re-organization of microstructural profile covariance (MPC) networks with increasingly resilient mental health outcomes.*** **A)** Top; Group differences in the Maturational index ($MI_{MPC;}$ FDR p<0.05 & 10,000 permutations, p<0.05) indicating a widespread negative shift (i.e., more disruptive or less conservative MPC development) in the group of individuals who developed towards more resilient outcomes (↑ΔSRS). Bottom; A negative shift for the ↑ΔSRS group can reflect three main scenarios: Less conservative development (left), more disruptive development (middle), or disruptive development in a region that exhibits neither disruptive nor conservative development in the full sample (right; tipping point). **B)** Contextualization of regions with a significant group difference (in any direction), revealing that differences in MI_{MPC} are more frequently located in Eulaminate cortex II & III, default mode areas, and regions exhibiting decoupled microstructural compared to functional development. **C)** Density plot of axis loadings per group, reflecting a more compressed axis in the group of individuals who developed towards more resilient outcomes. For scatter and density plots, the +ΔSRS group is depicted in purple and the -ΔSRS group in blue. Kon = Konicortex, Eu-I-III = Eulaminate I-III, Dys = Dysgranular, Ag = Agranular; DMN = Default mode network, FPN = Frontoparietal network, VAN = Ventral attention network, DAN = Dorsal attention network, SM = Sensorimotor, VIS = Visual.

Discussion

In the current study, we report that intra-individual trajectories of adolescent psychosocial functioning relative to environmental adversity are tied to ongoing myeloarchitectural and functional maturation of association cortices. Here, resilient and susceptible outcomes were operationalized as comparatively lower or higher levels of psychosocial distress in the face of psychosocial stressors, resulting in a continuous score that adjusts for variations in stressor exposure at different time points. We employed a dimensional approach aligning with previous studies that underscore psychosocial adversity as a pivotal transdiagnostic risk factor that is more predictive of overall psychopathology than discrete symptom domains [47,48]. Moreover, our longitudinal design puts emphasis on the dynamic nature of resilient functioning, combined with myeloarchitectural brain phenotypes that take regional variations along cortical depths into account. Thus, we provide nuanced and multimodal evidence that maturational trajectories of late-maturing association cortices are associated with changing abilities to adapt to psychosocial stressors during adolescence.

Enhanced anterolateral prefrontal myelination links to increasingly resilient psychosocial functioning

Investigating myelin trajectories revealed a positive association between ΔMT in anterolateral and orbitofrontal cortex and changes in stressor resilience scores. This finding converges with previous cross-sectional reports suggesting particular susceptibility of the ventral prefrontal cortex to environmental adversity [3,21,49] as well as a central role in resilient adaptation [47,50]. Here, we extend previous findings on cortical volumes and functional connectivity towards longitudinal myelin plasticity. A beneficial effect of enhanced prefrontal myelination may directly be linked to the optimization of adaptive cognitive strategies facilitating successful navigation in the ever-changing environment. That is, ongoing myelin plasticity fosters circuit modification and synchronization through a multitude of parallel mechanisms [18]. These may include regulatory influences on axon conductance to optimize the synchronization of spike arrivals [51,52], neuronal metabolism and excitability [53,54], and structural plasticity [14,55]. In the prefrontal cortex, the optimization of circuit efficiency is intricately linked to the maturation of cognitive functions such as executive functions and emotion regulation, and enhanced social and cognitive flexibility required for adaptation [56,57]. Conversely, attenuated prefrontal myelination and impaired executive control have been linked to transdiagnostic mental health impairments [58–60]. Schizophrenia rat models further suggest links between interneuron hypomyelination and cognitive inflexibility [61]. It is noteworthy that adolescents exhibiting increasingly susceptible outcomes in the present study did not surpass clinical thresholds. However, current findings indicate that cross-sectional associations between susceptibility to psychopathological spectra and prefrontal myeloarchitectural development described in patient and animal data can already be observed at the level of intra-individual variation in susceptibility. Lastly, alongside potential cognitive implications, psychosocial adversity likely elicits a physiological stress response activating the Hypothalamus-Pituitary-Adrenal axis. The ventral PFC is involved in and can recursively be affected by physiological stress responses through glucocorticoid-induced structural remodeling [62,63]. While the current data do not allow to test protective effects on a molecular level, it is possible that increased consolidation of connections through myelination may enhance physiological resistance to disadvantageous stressor-induced PFC re-modeling.

We probed whether varying levels of myeloarchitectural consolidation coincide with differences in functional network maturation of the identified anterolateral prefrontal region, indirectly suggesting a potential resistance to stressor-induced re-modeling. Indeed, we observed increasingly susceptible mental health outcomes to be linked not only to an attenuated rate of prefrontal myelination, but also to a segregation of prefrontal connectivity within abstract cognitive networks. Conversely, PFC

connectivity exhibited greater stability among individuals who developed towards more resilient psychosocial functioning. In normative development, most prefrontal sub-regions show decreases in global network embedding during childhood followed by a plateau towards early adulthood [64–66]. This pattern reflects a combination of increasing integration within networks that they are part of, such as the DMN and FPN, but a segregation from other networks such as the dorsal attention network. Here, the segregation of the anterolateral PFC region both globally and within the DMN and FPN in individuals manifesting increasingly susceptible outcomes suggests a closer tie to patterns reminiscent of earlier developmental stages in both prefrontal connectivity and mean myelin-sensitive MT. Together, increased longitudinal myelination of anterolateral prefrontal regions may link to facilitated adaptation to adversity by optimizing the efficiency of prefrontal cognitive circuits relevant to flexible adaptation and resistance to unfavorable re-modeling.

Synchronized re-organization of regions higher up the cytoarchitectonic and functional hierarchies are implicated in developing resilient psychosocial functioning

Brain alterations linked to both maturational and psychopathological cortical alterations have been proposed to occur in a network-like fashion rather than in isolation [36,37], underlining the importance of considering the embedding of local changes in a globally changing system. Therefore, we studied the cortical topology of synchronized maturation of intracortical profiles, to then probe whether areas exhibiting most pronounced re-organization during adolescence are more strongly implicated in trajectories of resilient psychosocial functioning. We described a maturational index reflecting age-related change as a function of baseline patterns and observed most profound re-organization in frontoparietal association cortices. The MI_{MPC} pattern aligned with a previously established principal axis of age-related MPC change that suggests fronto-parietal heteromodal cortex to differentiate most profoundly in synchronization with either dorsal/unimodal or ventral/paralimbic anchors [20]. Importantly, the microstructural maturational topology diverges to some extend from the maturational topology that has been previously described for functional networks [44]. Especially cognitive networks such as the FPN and DMN exhibited not only congruent disruptive development, but also a structure-function de-coupling marked by conservative MPC but disruptive FC development. Remodeling functional and structural connectivity partly independently has been assumed to sculpt functional specialization in transmodal association cortex critical for executive functions [34]. At the same time, it underlines the importance of multi-modal investigations when aiming to understand consequences of system-level maturation.

We observed associations between MI and changes in resilient psychosocial functioning in microstructural, and regionally confined effects in intrinsic functional data. Compared to individuals developing towards higher stressor susceptibility, adolescents developing towards more resilient outcomes exhibited a negative-shift in the microstructural MI_{MPC} across heteromodal association cortices. This negative-shift reflected both less conservative and more disruptive development. The observed reduction in conservative development was further highlighted by a compressed axis of MPC change for which less regions loaded towards the apices/anchors of the axis. In contrast to ΔSRS effects observed in MI_{MPC}, MI_{FC} effects were more locally concentrated in the bilateral prefrontal cortex and presented a positive rather than negative shift in MI_{FC} in individuals who became more resilient with age. That is, the +ΔSRS group exhibited less disruptive development in the PFC. This finding is complementary to microstructural maturational patterns associated with longitudinal change in resilient functioning and converges with the observation that increasingly resilient outcomes were associated with more maintained prefrontal functional connectivity (see **Figure 2C,** here reflected in attenuated re-organization). Previous work suggests regions that are most developmentally active during adolescence, primarily association cortices, to be most strongly implicated in mental health [1]. While we generally

observed effects in association cortices, this was not exclusive to regions exhibiting disruptive re-organization. In particular for the microstructural MI_{MPC}, effects associated with SRS changes were marked in temporal cortex, which in turn exhibited largely conservative development. Our results thus indicate that trajectories of resilient psychosocial functioning are linked to altered degrees of myeloarchitectural re-organization, however, this was independent from whether a region generally developed conservatively or disruptively.

Across analytical scales and imaging modalities included in this study, regions implicated in longitudinal change in resilient psychosocial functioning were characterized by their high position along cortical hierarchies of cytoarchitectonic complexity and functional network abstraction. That is, findings emerged predominantly in cytoarchitectonically complex Eulaminate-II and -III cortices, anatomically, and the DMN, functionally. Previous research suggests that structural differentiation of the DMN from networks involved in sensory-perceptual processing [45] facilitates the maturation of cognitive functions requiring abstraction from the immediate environment [56,57]. At the same time, DMN structure and functional connectivity are frequently implicated across psychiatric symptom domains, exposure to environmental adversity such as low socio-economic-status, but also to protective environmental factors such as positive parenting [67–69]. A prominent explanation for the recurring role of the DMN is its involvement in generating conceptual mental models of the self in its environment [70–73]. Such self-in-context models include self-referential processing, emotional reappraisal, assigning meaning to external events and interpreting their causes in reference to one's own narrative. Maladaptive internal models and inaccurate attributions of causality fostering negative interpretations of experiences have been considered transdiagnostic risk factors for mental health impairments [68,70]. Similarly, resilient or susceptible psychosocial trajectories may be tied to continuously evolving self-in-context representations. Here, ongoing DMN refinement may facilitate and stabilize beneficial self-referential mental narratives influencing adaptive strategies in the face environmental stressors.

Lastly, investigating both an average myelin proxy (i.e., regional MT) and a more nuanced approximation of intra-cortical profiles highlighted different facets of the associations between cortical maturation and change in stressor resilience. Yet, both angles support a beneficial role of myelin plasticity, reflected in a higher overall rate of (anterolateral prefrontal) myelin growth and, considering depth-specific measures, increased levels of microstructural re-organization. Across present analyses, individuals who developed towards more susceptible outcomes showed maturational profiles more closely tied to patterns associated with earlier stages of adolescence. Conversely, microstructural maturation in individuals with increasingly resilient outcomes appeared less constrained by existing patterns, potentially highlighting the necessity for adaptive alterations to enhance selected cognitive circuits. Overall, it is likely not only a matter of 'the more the better', but of parallel refinement processes taking place at multiple scales. Thus, current results demonstrate that adolescents show marked intra-individual variability in resilient psychosocial functioning relative to environmental adversity that is reflected in both local and systems-level brain maturational profiles.

Limitations, further considerations, & open questions

Our study takes a dimensional approach to environmental adversity exposure and psychosocial functioning. We acknowledge that differences exist in the brain correlates of both adversity type [49] and symptom domains [4]. However, we believe a dimensional approach increases ecological validity as included forms of adversity are highly clustered together in the general population [74], have been shown to be associated with overlapping brain structural correlates (dice coefficients up to 0.54; [3,49]), and are transdiagnostic predictors of overall psychopathology [47,48]. We further cannot extrapolate whether individuals stay on the trajectories analyzed here, and whether enhanced myelination is a prospective

predictor for adult mental health [48]. Next, our study does not allow to draw conclusions on the directionality of effects. It remains an open question whether reported brain maturational changes directly facilitate behaviors which in turn support advantageous outcomes, or whether favorable patterns of brain maturation are the result of environmental resilience factors such as a supportive social network [38,48,75]. On this note, resilient outcomes are assumed to rely on a multi-modal and multi-faceted construct, acknowledging the surrounding we live in, but also other psychological variables beyond symptomatology (such as positive affect, life satisfaction, personality traits). Thus, we cannot clearly disentangle the interaction of different intrinsic and extrinsic influences. The variety of factors affecting an individual's mental health are likely reflected in the variance not explained by our model, which predicts psychosocial distress solely from psychosocial adversity measures. Last, complementary to longitudinal approaches aiming to make prospective predictions of future mental health outcomes, our current work makes a case for tracking ongoing developmental trajectories for a better understanding of intra-individual variability in susceptibility to environmental risk factors at different time points during development.

Conclusion

The transition to adulthood is considered a particularly susceptible period for the emergence of mental health symptoms. In line with prior research proposing a central role of the protracted development of association cortices in susceptibility to psychiatric risk factors [19], the current work suggests that intra-individual change in psychosocial responses to environmental stressors is associated with the degree of myeloarchitectural plasticity and cortex-wide re-organization. The dynamic nature of myelin suggests a potential benefit of interventions that target deviant trajectories in at-risk adolescents. These may include increased exposure to environmental resilience factors such as a supportive social network [38,48], but also the facilitation of experience-dependent plasticity demonstrated in e.g. social/mental training [76].

Methods

Study sample

This study included 2245 adolescents and young adults aged 14 to 26 years (54% females; mean age = 19.06 ± 3.02y) from the NeuroScience in Psychiatry Network (NSPN; [77]). Participants were recruited in Cambridgeshire and north London in an accelerated longitudinal sampling design which balanced sex, ethnicity, and participant numbers in five age strata (14-15, 16-17, 18-19, 20-21, 22-25). All 2245 individuals were included in behavioral analyses (see **Supplementary Figure S8** for details on included sub-samples).

Our neuroimaging analyses of group-level developmental principles were based on a subsample (n = 199; 416 sessions) of adolescents who were invited to undergo longitudinal functional and structural neuroimaging assessments at baseline and a one year follow up, with a subsample of 26 subjects invited for an intermediate 6 months scan. Neuroimaging analyses studying intra- and inter-individual differences with respect to adaptivity were restricted to participants who had at least two structural (MT) and functional scans after quality control, and completed all questionnaires included in this study at two or more timepoints (*n* = 141; 346 sessions; age stratification at baseline: n = 34/34/22/37/14; 50.3% female; inter-scan interval = 1.26 ± 0.33y; **Supplementary Figure S8**). This study was conducted in accordance with U.K. National Health Service research governance standards and participants provided informed written consent during NSPN data acquisition.

Generation of stressor resilience scores

Stressor resilience scores (SRS) were generated in a three-step process (**Figure 1C**): 1) Computation of a general distress score (*n* = 1533), 2) prediction of psychosocial distress from environmental adversity measures (*n* = 712), and 3) extractions of residuals from the model for participants with repeated MRI and behavioral data (*n* = 141). To avoid leakage, steps 1 and 2 were based on independent subsamples (**Supplementary Figure S8**).

Psychosocial distress scores were based on self-report questionnaires spanning mental health domains for which emotional and behavioral symptoms tend to emerge during adolescence and are associated with commonly diagnosed mental disorders. Following previous work on latent mental health dimensions in NSPN [39], the following mental health domains and questionnaires were included: Depression (33-item Moods and Feelings Questionnaire; MFQ; [78]), generalized anxiety (including measures of social concerns, worry, physiological change; 28-item Revised Children's Manifest Anxiety Scale; RCMAS [79]), antisocial behaviours (11-item Antisocial Behaviour Questionnaire; ABQ), obsessive compulsive behavior (11-item Revised Leyton Obsessional Inventory; r-LOI; [80]), self-esteem (10-item Rosenberg Self-Esteem Questionnaire; RSE; [81]), psychotic-like experiences (Schizotypal Personality Questionnaire; SPQ; [82]), and mental well-being (14-item Warwick-Edinburgh Mental Well-Being Scale; WEMWBS; [83]). Please see supplementary information for details on the questionnaires. We applied a factor analysis (Matlab 2022b) aiming to derive one latent factor in 1533 individuals. This latent factor correlated highly (r = 0. 99) with the general distress score derived from previously reported Bi-factor models that additionally include five sub-factors [39]. In a separate subsample (*n* = 712), we then applied the derived item loadings to each individual's respective item scores. The sum of item scores multiplied by item loadings defined subject-level distress scores.

Conceptualizing relatively more resilient or susceptible outcomes as lower or higher than expected distress, respectively, given the adversity faced, we then predicted distress scores from

available adversity measures. These included: The Life Events Questionnaire (LEQ; [84]), Child Trauma Questionnaire (CTQ; [85]), Alabama Parenting Questionnaire (APQ; [86]), Measure of Parenting Style (MOPS; [87]), and socioeconomic status (as approximated by zip codes/IMD). See **Supplementary Methods** for details on included questionnaires. For the prediction, we used a random forest regression in a supervised machine learning approach implemented in sci-kit learn (v1.2.1, https://scikit-learn.org, in Python v3.10.9). We applied a nested cross-validation in which we left all sessions of one subject out in the outer scheme, i.e., 712 outer folds, and split the remaining data into 5 even groups for training, i.e., 5 inner folds, in each iteration. Performance was estimated based on mean absolute errors and parameter optimization was performed for the number of estimators (50, 100, 150, 200, 250, 300) and tree depth (5 to 15). We included a StandardScaler (z-scoring) to preprocess features within the cross-validation scheme.

Neuroimaging data acquisition

Magnetic Transfer data was acquired as a neuroimaging proxy of myelin content using a multi-parametric mapping (MPM) sequence [22] on three identical 3T Siemens MRI Scanners (Magnetom TIM Trio) in Cambridge (2) and London (1). A standard 32-channel radio-frequency (RF) receive head coil and RF body coil for transmission were used. Anatomical and functional data were acquired on the same day.

Myelin-sensitive MRI

MPM comprised three multi-echo 3D FLASH scans: predominant T1-weighting (repetition time (TR) = 18.7 ms, flip angle = 20°), and predominant proton density (PD) and MT-weighting (TR= 23.7 ms; flip angle = 6°). To achieve MT-weighting, an off-resonance Gaussian-shaped RF pulse (duration = 4 ms, nominal flip angle = 220˚, frequency offset from water resonance = 2 kHz) was applied prior to the excitation. For MT weighted acquisition, several gradient echoes were recorded with alternate readout polarity at six equidistant echo durations (TE) between 2.2 and 14.7 ms. The longitudinal relaxation rate and MT signal are separated by the MT saturation parameter, creating a semi-quantitative measurement that is resistant to field inhomogeneities and relaxation times [22,88]. Further acquisition parameters: 1 mm isotropic resolution, 176 sagittal partitions, field of view (FOV) = 256×240 mm, matrix = 256×240×176, parallel imaging using GRAPPA factor two in phase-encoding (PE) direction (AP), 6/8 partial Fourier in partition direction, non-selective RF excitation, readout bandwidth BW = 425 Hz/pixel, RF spoiling phase increment = 50˚. The acquisition time was approx. 25 min, during which participants wore ear protection and were instructed not to move and rest.

Resting-state functional MRI

Resting-state functional MRI (fMRI) data were acquired using a multiecho echo-planar imaging sequence (TR = 2.42 s; GRAPPA with acceleration factor = 2; flip angle = 90°; matrix size = 64×64×34; FOV = 240 × 240 mm; in plane resolution = 3.75 mm×3.75 mm; slice thickness = 3.75 mm with 10% gap, sequential slice acquisition, 34 oblique slices; bandwidth, 2368 Hz/pixel; TE = 13, 30.55, and 48.1 ms.

Neuroimaging data preprocessing

Microstructure

Surface reconstruction was performed on T1w data using the Freesurfer _recon-all_ command (v.5.3.0; [89]). Briefly, the pipeline performs non-uniformity correction, projection to Talairach space, intensity normalization, skull stripping, automatic tissue segmentation, and construction of the gray/white interface and the pial surface. Surface reconstructions were visually inspected and edited by adding control points if required, or excluded if still poor following editing. MT images were co-registered with reconstructed surfaces and 12 equivolumetric cortical surfaces were generated within the cortex (i.e., between the pial and white surface; [90]). The equivolumetric model takes cortical folding into account by manipulating the Euclidean distance (ρ) between intracortical surfaces, thereby preserving the fractional volume between pairs of surfaces:

$$\rho = \frac{1}{A(out) - A(in)} \times (A(in) + \sqrt{\alpha A^2(ou)} + (1-\propto)A^2(in)$$

α = a fraction of the total volume of the segment accounted for by the surface; A_{out} and A_{in} = the surface areas of outer and inner cortical surfaces, respectively.

The outer two surfaces were excluded to avoid potential partial volume effects (PVE) and MT intensities were extracted from 10 cortical depths at each vertex. In addition, depth-specific PVEs caused by cerebrospinal fluid (CSF) were corrected for using a mixed tissue class model [91]. To this end, a linear model was fitted to each node at all 10 depths:

$$MT(n,s) \sim b_0 + b_1 CSF(n,s)$$

where n = node, s = surface. Derived CSF-corrected MT values reflect the sum of residuals:

$$MTc(n,s) = T1(n,s) - (b_0 + b_1 CSF(n,s))$$

and original group averaged MT.

Last, vertices were averaged within 360 bilateral cortical parcels using the Human Connectome Project (HCP) parcellation atlas that was mapped from standard fsaverage space to each participant's native space using surface-based registration [90,92].

Resting-state functional MRI

Multi-echo independent component analysis (ME-ICA; [93,94]) was applied to the fMRI data to isolate and remove variance caused by sources that do not scale linearly with the TR within the time series and are therefore assumed not to represent the blood oxygenation level dependent (BOLD) contrast. Variance in cerebrospinal fluid was estimated based on ventricular time series and regressed from parenchymal time series via Analysis of Functional NeuroImages (AFNI; [95]). Data was parcellated into the same 360 bilateral HCP cortical regions applied to structural data within which regional time series were averaged across voxels of each respective parcel. Moreover, a band-pass-filter (range: 0.025 to 0.111 Hz [96]) was

applied to the regional time series using discrete wavelet transform. Following quality control, regional time series were z-scored and 30 regions, mainly in paralimbic areas, were excluded due to low z-scores ($Z < 1.96$) in at least one participant. A functional connectivity (FC) matrix was generated for each subject by computing Pearson's correlation coefficients between all 330 remaining parcels, yielding a 330×330 matrix. Correlation coefficients were then z-transformed by Fisher's transformation [97]). Hence, FC units represent standard deviations of the normal distribution. Lastly, to avoid any residual effects of motion on FC, each edge/Z-score was regressed on each participant's mean frame-wise displacement. All further analyses were based on derived motion-corrected Z-scores (i.e., the residuals of this regression).

In total, 36 scans were excluded due to high in-scanner motion [mean framewise displacement (FD) > 0.3 mm or maximum FD > 1.3 mm], poor surface reconstructions, co-registration errors, and/or extensive fMRI dropout.

Intra-individual change

Intra-individual change in mean and layer-wise MT, as well as resting-state functional connectivity (FC), was assessed by calculating the Δ between first and last MRI sessions: MT_{T2}-MT_{T1} or FC_{T2}-FC_{T1} respectively, for each parcel. Δs were winsorized to +/- 3SD to account for outliers.

Association between myeloarchitectural and intrinsic functional maturation and change in SRS

The association between ΔSRS and ΔMT was assessed by applying a general linear model to each parcel:

$$\Delta MT(parcel) \sim 1 + \beta_{\Delta SRS} * \Delta SRS + \beta_{mean\ SRS} * mean\ SRS + \beta_{age} * age + \beta_{sex} * sex + \beta_{site} * site + \epsilon$$

Models were fitted in SurfStat [98] (Matlab 2022b) adjusting for mean age (i.e., $(Age_{baseline} + Age_{follow\ up})/2$) and mean SRS (i.e., $(SRS_{baseline} + SRS_{follow\ up})/2$) across sessions, sex, and site. Before fitting the model, we adjusted ΔSRS and ΔMT for inter-session-intervals, which varied between participants, by fitting linear regressions of Δage. This was done separately for imaging and behavioral data to adjust for the fact that behavioral and imaging data were mostly not collected on the same day. Significance was assessed by non-linear permutation testing (10.000 permutations of Δ and mean SRS and FDR correction of derived p-values at $\alpha < 0.05$). We then stratified the unthresholded t-map according to a cytoarchitectonic map defining six dominant cortical types [28], to reveal potential systematic links between cortical architecture and ΔSRS effects.

We ran two post-hoc analyses based on the region of interest (ROI) defined by parcels that show a significant ΔSRS*ΔMT association. First, we tested whether significant associations between ΔSRS and ΔMT were layer-specific by fitting the same linear model to MT values at each of the 10 surfaces, rather than the mean across surfaces. This was done to reveal a potential specificity of effects based on cortical depth, not to statistically confirm the observed association again. Next, we addressed the question of whether regions showing differences in ΔMT as a function of ΔSRS also exhibit different functional connectivity. To this end, we computed global FC of the ROI as degree centrality (i.e., the sum of all connections) as well as a seed-based FC analysis defining the ROI as a seed. As described for the ΔMT analysis, we regressed out the effects of inter-session intervals, fitted the same linear model as

described above, and assessed significance of the seed-based analysis by non-linear permutation testing (10,000 permutations of Δ and mean SRS + FDR correction of derived *p*-values at $\alpha < 0.05$). Last, we stratified the resulting t-map according to the Yeo 7 Network Atlas [46] to reveal systematic effects within specific intrinsic functional networks.

System-level maturation

We studied systems-level maturation based on both myeloarchitectural and functional data. In order to assess the cortical topology of MT maturation, we computed a microstructural profile covariance (MPC) matrix and studied its change with age. MPC is based on myeloarchitectural profiles across cortical depths and is generated via partial correlations between depth-wise MT profiles of two given regions, corrected for the mean MT signal across surfaces. An underlying assumption of this approach is that inter-regional similarity predicts axonal cortico-cortical connectivity [33,99,100]. MPC has previously been shown to align well with post-mortem assessments of inter-regional microstructural similarity [30], and depth-dependent shifts in cytoarchitectonic features such as cell densities or myelin characteristics have been linked to architectural [101] complexity and cortical hierarchy [102].

First, we computed a microstructural and functional Maturational Index (MI), which has been shown to be a robust marker for adolescent modes of re-organization [44] sensitive to individual differences [103] in functional connectivity. To compute the MI, LMEs were fitted to each edge of the MPC and FC matrices, assessing effects of age and including sex, site, and repeated measures of the same individual in the model:

$$\mathrm{MRI}(k,j) \sim 1 + \beta_{\mathrm{age}} * \mathrm{age} + \beta_{\mathrm{sex}} * \mathrm{sex} + \beta_{\mathrm{site}} * \mathrm{site} + \gamma_{\mathrm{subject}} * (1|\mathrm{subject}) + \epsilon$$

Where k and j are two nodes of the matrix. The MI captures the signed Spearman's correlation between predicted baseline patterns, at age 14, and rate of change, age 14-26, of all edges that connect a given node to all other nodes. Thus, it reflects a re-organization of network embedding.

Baseline values at age 14 for each group (+ΔSRS/-ΔSRS), $\mathrm{MRI}14_{\mathrm{group}}$, were extracted for MPC and FC matrices as follows:

$$\mathrm{MRI}14_{\mathrm{group}} = 1 + \beta_{\mathrm{age}} * 14 + \beta_{\mathrm{age}} * 14 + \beta_{\mathrm{sex}} * (1/2) + \beta_{\mathrm{site1}} * (1/3) + \beta_{\mathrm{site2}} * (1/3)$$

Whereas the rate of change $\mathrm{MPC}_{14\text{-}26}$ or $\mathrm{FC}_{14\text{-}26}$ simply reflects the β-coefficient of age:

$$\mathrm{MRI}_{14\text{-}26}(k,j) = \beta_{\mathrm{age}}$$

At each node, we then computed the row-wise Spearman's ρ between ranked extracted parameters reflecting baseline and change parameters of all edges (i.e., 360 for MPC, 330 for FC) of a specific node. A positive correlation indicates that a given region's edges that were already similar in either their myeloarchitectural or functional profile became more similar with development, this is termed 'conservative' development. Conversely, a negative correlation reflects re-organization, edges that were similar at baseline differentiate, or edges that were dissimilar at baseline integrate, which is termed 'disruptive' development. We computed normative MIs for MPC and FC across all participants (n =

199) using all existing sessions (416 sessions). To probe convergence and divergence of structural compared to functional maturational modes, we further tested overlaps between regional MIs (individually thresholded at pFDR < 0.05).

Next, we contextualized the MI_{MPC} with a previously established measure of global organization of microstructural maturation: The MPC principal axis of age effects [20]. To this end, we applied the same LME defined above:

$$MPC(k,j) \sim 1 + \beta_{age} * age + \beta_{sex} * sex + \beta_{site} * site + \gamma_{subject} * (1|subject) + \epsilon$$

to each edge of the MPC matrix, assessing the main effect of age on inter-regional microstructural similarities. Diffusion map embedding was then applied to the matrix of *t*-values (thresholded at 90%), revealing a cortex-wide organizational axis of synchronized age effects. Regions with a similar loading on this axis are similarly embedded in a network of inter-regional synchronization of age effects, whereas regions at the apices of the axis show maximally different change patterns.

Group-level differences in system-level maturation

Last, we aimed to study differences in system-level maturation associated with intra-individual changes in adaptivity. As the MI is computed from parameters extracted from group-level general linear models, it was required to split the sample into two groups. Hence, the sample was split into adolescents who showed increasingly resilient outcomes (+ΔSRS; *n*=81, 193 sessions; 48% female, 18.93±2.81y at baseline) and adolescents who became more susceptible with age (-ΔSRS *n*=60; 153 sessions; 53% female, 18.84± 2.87y at baseline). MIs were computed for each group separately, and resulting maps were subtracted from each other (+ΔSRS - (-ΔSRS)). Significance was tested using two approaches that were combined for thresholding: 1) We first applied Z-tests testing for significant differences between the correlation coefficients, i.e., the difference between group MIs divided by the SE of the difference in MIs, as has previously been done [103].

$$z = \frac{MI_{+\Delta SRS} - MI_{-\Delta SRS}}{SE_{MI_{+\Delta SRS} - MI_{-\Delta SRS}}} = \frac{MI_{+\Delta SRS} - MI_{-\Delta SRS}}{\sqrt{SE_{MI_{+\Delta SRS}}{}^2 + SE_{MI_{-\Delta SRS}}{}^2}}$$

Derived p-values were FDR-corrected at pFDR < 0.05.

2) Next, to control for the effects of sampling bias and potential effects of differences in group size or demographics, we performed non-parametric permutation testing, shuffling group allocation 10,000 times while considering age and sex distributions as well as group size differences (see **Supplementary Figure S9**). Finally, we depicted group differences as significant only if they were significant in both FDR-corrected p-values derived from Z-tests (p<0.05), and non-parametric permutation testing (p<0.05).

Data availability

Preprocessed microstructural profiles and stressor resilience scores are available via GitHub: https://github.com/CNG-LAB/cngopen/tree/main/adolescent_resilience/data. Preprocessed functional connectivity matrices have previously been published under: https://zenodo.org/records/6390852. Generally, access to NSPN data can be requested here: https://portal.ide-cam.org.uk/overview/6/managed or https://www.repository.cam.ac.uk/handle/1810/264350

Code availability

Custom code generated for this project was made publicly available under https://github.com/CNG-LAB/cngopen/tree/main/adolescent_resilience/ScrFun. Our analysis code makes use of open software: Gradient mapping analyses were carried out using BrainSpace (v. 0.1.2; https://brainspace.readthedocs.io/en/latest/)

and surface visualizations were based on code from the ENIGMA Toolbox (v.1.1.3; https://enigma-toolbox.readthedocs.io/en/latest/; [104]) in combination with ColorBrewer (v. 1.0.0; https://github.com/scottclowe/cbrewer2). Statistical analyses were carried out using SurfStat (https://www.math.mcgill.ca/keith/surfstat/). Equivolumetric surfaces were computed using code from: https://github.com/MICA-MNI/micaopen/tree/master/a_moment_of_change [20]. Z-tests were performed using the compare correlation coefficients function (Sisi Ma (2024). compare_correlation_coefficients (https://www.mathworks.com/matlabcentral/fileexchange/44658-compare_correlation_coefficients).

Acknowledgements

Many scientists contributed to the NSPN consortium but did not take active part in the writing of this report. A full list of contributors to NSPN is available in the supplementary material. The authors would like to express their gratitude to the open science initiatives that made this work possible. *Funding:* MDH was funded by the German Federal Ministry of Education and Research (BMBF) and the Max Planck Society. L.D. was supported by a Gates Cambridge Scholarship. S.L.V. was supported by the Max Planck Society through the Otto Hahn Award and the Helmholtz International BigBrain Analytics and Learning Laboratory (Hiball).

References

1. Paus T, Keshavan M, Giedd JN. Why do many psychiatric disorders emerge during adolescence? *Nat Rev Neurosci*. 2008;9(12):947-957. doi:10.1038/nrn2513
2. Parkes L, Moore TM, Calkins ME, et al. Transdiagnostic dimensions of psychopathology explain individuals' unique deviations from normative neurodevelopment in brain structure. *Transl Psychiatry*. 2021;11(1):1-13. doi:10.1038/s41398-021-01342-6
3. Holz NE, Zabihi M, Kia SM, et al. A stable and replicable neural signature of lifespan adversity in the adult brain. *Nat Neurosci*. Published online August 21, 2023:1-10. doi:10.1038/s41593-023-01410-8
4. Yu G, Liu Z, Wu X, et al. Common and disorder-specific cortical thickness alterations in internalizing, externalizing and thought disorders during early adolescence: an Adolescent Brain and Cognitive Development study. *J Psychiatry Neurosci*. 2023;48(5):E345-E356. doi:10.1503/jpn.220202
5. Ziegler G, Hauser TU, Moutoussis M, et al. Compulsivity and impulsivity traits linked to attenuated developmental frontostriatal myelination trajectories. *Nat Neurosci*. 2019;22(6):992-999. doi:10.1038/s41593-019-0394-3
6. Hoppen TH, Morina N. The prevalence of PTSD and major depression in the global population of adult war survivors: a meta-analytically informed estimate in absolute numbers. *Eur J Psychotraumatology*. 2019;10(1):1578637. doi:10.1080/20008198.2019.1578637
7. Kalisch R, Baker DG, Basten U, et al. The resilience framework as a strategy to combat stress-related disorders. *Nat Hum Behav*. 2017;1(11):784-790. doi:10.1038/s41562-017-0200-8
8. Kessler RC, Aguilar-Gaxiola S, Alonso J, et al. Trauma and PTSD in the WHO World Mental Health Surveys. *Eur J Psychotraumatology*. 2017;8(sup5):1353383. doi:10.1080/20008198.2017.1353383
9. Eaton S, Cornwell H, Hamilton-Giachritsis C, Fairchild G. Resilience and young people's brain structure, function and connectivity: A systematic review. *Neurosci Biobehav Rev*. 2022;132:936-956. doi:10.1016/j.neubiorev.2021.11.001
10. van der Werff SJA, van den Berg SM, Pannekoek JN, Elzinga BM, van der Wee NJA. Neuroimaging resilience to stress: a review. *Front Behav Neurosci*. 2013;7:39. doi:10.3389/fnbeh.2013.00039
11. Feder A, Fred-Torres S, Southwick SM, Charney DS. The Biology of Human Resilience: Opportunities for Enhancing Resilience Across the Life Span. *Biol Psychiatry*. 2019;86(6):443-453. doi:10.1016/j.biopsych.2019.07.012
12. Malhi GS, Das P, Bell E, Mattingly G, Mannie Z. Modelling resilience in adolescence and adversity: a novel framework to inform research and practice. *Transl Psychiatry*. 2019;9(1):316. doi:10.1038/s41398-019-0651-y
13. Stainton A, Chisholm K, Kaiser N, et al. Resilience as a multimodal dynamic process. *Early Interv Psychiatry*. 2019;13(4):725-732. doi:10.1111/eip.12726
14. Zemmar A, Chen CC, Weinmann O, et al. Oligodendrocyte- and Neuron-Specific Nogo-A Restrict Dendritic Branching and Spine Density in the Adult Mouse Motor Cortex. *Cereb Cortex*. 2018;28(6):2109-2117. doi:10.1093/cercor/bhx116
15. Giedd JN, Blumenthal J, Jeffries NO, et al. Brain development during childhood and adolescence: a longitudinal MRI study. *Nat Neurosci*. 1999;2(10):861-863. doi:10.1038/13158
16. Paus T. Growth of white matter in the adolescent brain: myelin or axon? *Brain Cogn*. 2010;72(1):26-35. doi:10.1016/j.bandc.2009.06.002
17. Mount CW, Monje M. Wrapped to Adapt: Experience-Dependent Myelination. *Neuron*. 2017;95(4):743-756. doi:10.1016/j.neuron.2017.07.009
18. Xin W, Chan JR. Myelin plasticity: sculpting circuits in learning and memory. *Nat Rev*

Neurosci. 2020;21(12):682-694. doi:10.1038/s41583-020-00379-8
19. Sydnor VJ, Larsen B, Bassett DS, et al. Neurodevelopment of the association cortices: Patterns, mechanisms, and implications for psychopathology. *Neuron*. 2021;109(18):2820-2846. doi:10.1016/j.neuron.2021.06.016
20. Paquola C, Bethlehem RA, Seidlitz J, et al. Shifts in myeloarchitecture characterise adolescent development of cortical gradients. *eLife*. 2019;8. doi:10.7554/elife.50482
21. Larsen B, Sydnor VJ, Keller AS, Yeo BTT, Satterthwaite TD. A critical period plasticity framework for the sensorimotor–association axis of cortical neurodevelopment. *Trends Neurosci*. 2023;0(0). doi:10.1016/j.tins.2023.07.007
22. Weiskopf N, Suckling J, Williams G, et al. Quantitative multi-parameter mapping of R1, PD*, MT, and R2* at 3T: a multi-center validation. *Front Neurosci*. 2013;7. doi:https://doi.org/10.3389/fnins.2013.00095
23. Mancini M, Karakuzu A, Cohen-Adad J, Cercignani M, Nichols TE, Stikov N. An interactive meta-analysis of MRI biomarkers of myelin. *eLife*. 2020;9:e61523. doi:10.7554/eLife.61523
24. Odrobina EE, Lam TYJ, Pun T, Midha R, Stanisz GJ. MR properties of excised neural tissue following experimentally induced demyelination. *NMR Biomed*. 2005;18(5):277-284. doi:10.1002/nbm.951
25. Paquola C, Hong SJ. The Potential of Myelin-Sensitive Imaging: Redefining Spatiotemporal Patterns of Myeloarchitecture. *Biol Psychiatry*. 2023;93(5):442-454. doi:10.1016/j.biopsych.2022.08.031
26. Whitaker KJ, Vértes PE, Romero-Garcia R, et al. Adolescence is associated with genomically patterned consolidation of the hubs of the human brain connectome. *Proc Natl Acad Sci*. 2016;113(32):9105-9110. doi:10.1073/pnas.1601745113
27. Schmierer K, Tozer DJ, Scaravilli F, et al. Quantitative magnetization transfer imaging in postmortem multiple sclerosis brain. *J Magn Reson Imaging*. 2007;26(1):41-51. doi:10.1002/jmri.20984
28. García-Cabezas MÁ, Zikopoulos B, Barbas H. The Structural Model: a theory linking connections, plasticity, pathology, development and evolution of the cerebral cortex. *Brain Struct Funct*. 2019;224(3):985-1008. doi:10.1007/s00429-019-01841-9
29. Barbas H, Rempel-Clower N. Cortical structure predicts the pattern of corticocortical connections. *Cereb Cortex*. 1997;7(7):635-646. doi:10.1093/cercor/7.7.635
30. Paquola C, Vos de Wael RV, Wagstyl K, et al. Microstructural and functional gradients are increasingly dissociated in transmodal cortices. *PLOS Biol*. 2019;17(5):e3000284.
31. Valk SL, Xu T, Paquola C, et al. Genetic and phylogenetic uncoupling of structure and function in human transmodal cortex. *Nat Commun*. 2022;13(1):2341. doi:10.1038/s41467-022-29886-1
32. Paquola C, Garber M, Frässle S, et al. *The Unique Cytoarchitecture and Wiring of the Human Default Mode Network*. Neuroscience; 2021. doi:10.1101/2021.11.22.469533
33. Saberi A, Paquola C, Wagstyl K, et al. The regional variation of laminar thickness in the human isocortex is related to cortical hierarchy and interregional connectivity. *PLOS Biol*. 2023;21(11):e3002365. doi:10.1371/journal.pbio.3002365
34. Baum GL, Cui Z, Roalf DR, et al. Development of structure–function coupling in human brain networks during youth. *Proc Natl Acad Sci*. 2020;117(1):771-778. doi:10.1073/pnas.1912034117
35. Paquola C, Amunts K, Evans A, Smallwood J, Bernhardt B. Closing the mechanistic gap: the value of microarchitecture in understanding cognitive networks. *Trends Cogn Sci*. 2022;26(10):873-886. doi:10.1016/j.tics.2022.07.001
36. Di Martino A, Fair DA, Kelly C, et al. Unraveling the Miswired Connectome: A Developmental Perspective. *Neuron*. 2014;83(6):1335-1353.

doi:10.1016/j.neuron.2014.08.050
37. Hettwer MD, Larivière S, Park BY, et al. Coordinated cortical thickness alterations across six neurodevelopmental and psychiatric disorders. *Nat Commun*. 2022;13(1):6851. doi:10.1038/s41467-022-34367-6
38. Van Harmelen AL, Kievit RA, Ioannidis K, et al. Adolescent friendships predict later resilient functioning across psychosocial domains in a healthy community cohort. *Psychol Med*. 2017;47(13):2312-2322. doi:10.1017/S0033291717000836
39. St Clair MC, Neufeld S, Jones PB, et al. Characterising the latent structure and organisation of self-reported thoughts, feelings and behaviours in adolescents and young adults. *PLOS ONE*. 2017;12(4):e0175381. doi:10.1371/journal.pone.0175381
40. Bowes L, Maughan B, Caspi A, Moffitt TE, Arseneault L. Families promote emotional and behavioural resilience to bullying: evidence of an environmental effect. *J Child Psychol Psychiatry*. 2010;51(7):809-817. doi:10.1111/j.1469-7610.2010.02216.x
41. Collishaw S, Hammerton G, Mahedy L, et al. Mental health resilience in the adolescent offspring of parents with depression: a prospective longitudinal study. *Lancet Psychiatry*. 2016;3(1):49-57. doi:10.1016/S2215-0366(15)00358-2
42. Sapouna M, Wolke D. Resilience to bullying victimization: the role of individual, family and peer characteristics. *Child Abuse Negl*. 2013;37(11):997-1006. doi:10.1016/j.chiabu.2013.05.009
43. Miller-Lewis LR, Searle AK, Sawyer MG, Baghurst PA, Hedley D. Resource factors for mental health resilience in early childhood: An analysis with multiple methodologies. *Child Adolesc Psychiatry Ment Health*. 2013;7(1):6. doi:10.1186/1753-2000-7-6
44. Váša F, Romero-Garcia R, Kitzbichler MG, et al. Conservative and disruptive modes of adolescent change in human brain functional connectivity. *Proc Natl Acad Sci*. 2020;117(6):3248-3253. doi:10.1073/pnas.1906144117
45. Park B yong, Paquola C, Bethlehem RAI, et al. Adolescent development of multiscale structural wiring and functional interactions in the human connectome. *Proc Natl Acad Sci*. 2022;119(27):e2116673119. doi:10.1073/pnas.2116673119
46. Yeo BT, Krienen FM, Sepulcre J, et al. The organization of the human cerebral cortex estimated by intrinsic functional connectivity. *J Neurophysiol*. Published online 2011.
47. Keyes KM, Eaton NR, Krueger RF, et al. Childhood maltreatment and the structure of common psychiatric disorders. *Br J Psychiatry J Ment Sci*. 2012;200(2):107-115. doi:10.1192/bjp.bp.111.093062
48. McLaughlin KA, Colich NL, Rodman AM, Weissman DG. Mechanisms linking childhood trauma exposure and psychopathology: a transdiagnostic model of risk and resilience. *BMC Med*. 2020;18(1):96. doi:10.1186/s12916-020-01561-6
49. Pollok TM, Kaiser A, Kraaijenvanger EJ, et al. Neurostructural traces of early life adversities: A meta-analysis exploring age- and adversity-specific effects. *Neurosci Biobehav Rev*. 2022;135:104589. doi:10.1016/j.neubiorev.2022.104589
50. van der Werff SJA, van den Berg SM, Pannekoek JN, Elzinga BM, van der Wee NJA. Neuroimaging resilience to stress: a review. *Front Behav Neurosci*. 2013;7:39. doi:10.3389/fnbeh.2013.00039
51. Ford MC, Alexandrova O, Cossell L, et al. Tuning of Ranvier node and internode properties in myelinated axons to adjust action potential timing. *Nat Commun*. 2015;6(1):8073. doi:10.1038/ncomms9073
52. Kato D, Wake H, Lee PR, et al. Motor learning requires myelination to reduce asynchrony and spontaneity in neural activity. *Glia*. 2020;68(1):193-210. doi:10.1002/glia.23713
53. Larson VA, Mironova Y, Vanderpool KG, et al. Oligodendrocytes control potassium accumulation in white matter and seizure susceptibility. *eLife*. 2018;7:e34829. doi:10.7554/eLife.34829

54. Xin W, Mironova YA, Shen H, et al. Oligodendrocytes Support Neuronal Glutamatergic Transmission via Expression of Glutamine Synthetase. *Cell Rep*. 2019;27(8):2262-2271.e5. doi:10.1016/j.celrep.2019.04.094
55. Wang F, Ren SY, Chen JF, et al. Myelin degeneration and diminished myelin renewal contribute to age-related deficits in memory. *Nat Neurosci*. 2020;23(4):481-486. doi:10.1038/s41593-020-0588-8
56. Nelson EE, Guyer AE. The development of the ventral prefrontal cortex and social flexibility. *Dev Cogn Neurosci*. 2011;1(3):233-245. doi:10.1016/j.dcn.2011.01.002
57. Teffer K, Semendeferi K. Human prefrontal cortex. In: *Progress in Brain Research*. Vol 195. Elsevier; 2012:191-218. doi:10.1016/B978-0-444-53860-4.00009-X
58. Chini M, Hanganu-Opatz IL. Prefrontal Cortex Development in Health and Disease: Lessons from Rodents and Humans. *Trends Neurosci*. 2021;44(3):227-240. doi:10.1016/j.tins.2020.10.017
59. Etkin A, Gyurak A, O'Hara R. A neurobiological approach to the cognitive deficits of psychiatric disorders. *Dialogues Clin Neurosci*. 2013;15(4):419.
60. Knowles JK, Batra A, Xu H, Monje M. Adaptive and maladaptive myelination in health and disease. *Nat Rev Neurol*. 2022;18(12):735-746. doi:10.1038/s41582-022-00737-3
61. Maas DA, Eijsink VD, Spoelder M, et al. Interneuron hypomyelination is associated with cognitive inflexibility in a rat model of schizophrenia. *Nat Commun*. 2020;11(1):2329. doi:10.1038/s41467-020-16218-4
62. McEwen BS. Physiology and Neurobiology of Stress and Adaptation: Central Role of the Brain. *Physiol Rev*. Published online July 1, 2007. doi:10.1152/physrev.00041.2006
63. McEwen BS, Nasca C, Gray JD. Stress Effects on Neuronal Structure: Hippocampus, Amygdala, and Prefrontal Cortex. *Neuropsychopharmacology*. 2016;41(1):3-23. doi:10.1038/npp.2015.171
64. Lopez KC, Kandala S, Marek S, Barch DM. Development of Network Topology and Functional Connectivity of the Prefrontal Cortex. *Cereb Cortex*. 2020;30(4):2489-2505. doi:10.1093/cercor/bhz255
65. Sherman LE, Rudie JD, Pfeifer JH, Masten CL, McNealy K, Dapretto M. Development of the Default Mode and Central Executive Networks across early adolescence: A longitudinal study. *Dev Cogn Neurosci*. 2014;10:148-159. doi:10.1016/j.dcn.2014.08.002
66. Stevens MC, Pearlson GD, Calhoun VD. Changes in the interaction of resting-state neural networks from adolescence to adulthood. *Hum Brain Mapp*. 2009;30(8):2356-2366. doi:10.1002/hbm.20673
67. Whittle S, Vijayakumar N, Simmons JG, et al. Role of Positive Parenting in the Association Between Neighborhood Social Disadvantage and Brain Development Across Adolescence. *JAMA Psychiatry*. 2017;74(8):824-832. doi:10.1001/jamapsychiatry.2017.1558
68. Rebello K, Moura LM, Pinaya WHL, Rohde LA, Sato JR. Default Mode Network Maturation and Environmental Adversities During Childhood. *Chronic Stress*. 2018;2:2470547018808295. doi:10.1177/2470547018808295
69. Doucet GE, Janiri D, Howard R, O'Brien M, Andrews-Hanna JR, Frangou S. Transdiagnostic and disease-specific abnormalities in the default-mode network hubs in psychiatric disorders: A meta-analysis of resting-state functional imaging studies. *Eur Psychiatry*. 2020;63(1):e57. doi:10.1192/j.eurpsy.2020.57
70. Koban L, Gianaros PJ, Kober H, Wager TD. The self in context: brain systems linking mental and physical health. *Nat Rev Neurosci*. 2021;22(5):309-322. doi:10.1038/s41583-021-00446-8
71. Seth AK. Interoceptive inference, emotion, and the embodied self. *Trends Cogn Sci*. 2013;17(11):565-573. doi:10.1016/j.tics.2013.09.007
72. Friston K. The free-energy principle: a unified brain theory? *Nat Rev Neurosci*. 2010;11(2):127-138. doi:10.1038/nrn2787

73. Barrett LF. The theory of constructed emotion: an active inference account of interoception and categorization. *Soc Cogn Affect Neurosci*. 2017;12(1):1-23. doi:10.1093/scan/nsw154
74. Green JG, McLaughlin KA, Berglund PA, et al. Childhood Adversities and Adult Psychiatric Disorders in the National Comorbidity Survey Replication I: Associations With First Onset of DSM-IV Disorders. *Arch Gen Psychiatry*. 2010;67(2):113-123. doi:10.1001/archgenpsychiatry.2009.186
75. Reiter AMF, Moutoussis M, Vanes L, et al. Preference uncertainty accounts for developmental effects on susceptibility to peer influence in adolescence. *Nat Commun*. 2021;12(1):3823. doi:10.1038/s41467-021-23671-2
76. Valk SL, Kanske P, Park B yong, et al. Functional and microstructural plasticity following social and interoceptive mental training. Nord CL, Makin TR, Sui YV, Kim SG, eds. *eLife*. 2023;12:e85188. doi:10.7554/eLife.85188
77. Kiddle B, Inkster B, Prabhu G, et al. Cohort Profile: The NSPN 2400 Cohort: a developmental sample supporting the Wellcome Trust NeuroScience in Psychiatry Network. *Int J Epidemiol*. 2018;47(1):18-19g. doi:10.1093/ije/dyx117
78. Costello EJ, Angold A. Scales to Assess Child and Adolescent Depression: Checklists, Screens, and Nets. *J Am Acad Child Adolesc Psychiatry*. 1988;27(6):726-737. doi:10.1097/00004583-198811000-00011
79. Reynolds CR, Richmond BO. What I think and feel: a revised measure of children's manifest anxiety. *J Abnorm Child Psychol*. 1978;6(2):271-280. doi:10.1007/BF00919131
80. Bamber D, Tamplin A, Park RJ, Kyte ZA, Goodyer IM. Development of a short leyton obsessional inventory for children and adolescents. *J Am Acad Child Adolesc Psychiatry*. 2002;41(10):1246-1252. doi:10.1097/00004583-200210000-00015
81. Rosenberg M. The measurement of self-esteem, Society and the adolescent self-image. *Princeton*. Published online 1965:16-36.
82. Raine A. The SPQ: a scale for the assessment of schizotypal personality based on DSM-III-R criteria. *Schizophr Bull*. 1991;17(4):555-564. doi:10.1093/schbul/17.4.555
83. Tennant R, Hiller L, Fishwick R, et al. The Warwick-Edinburgh Mental Well-being Scale (WEMWBS): development and UK validation. *Health Qual Life Outcomes*. 2007;5:63. doi:10.1186/1477-7525-5-63
84. Goodyer IM, Herbert J, Tamplin A, Altham PM. Recent life events, cortisol, dehydroepiandrosterone and the onset of major depression in high-risk adolescents. *Br J Psychiatry J Ment Sci*. 2000;177:499-504. doi:10.1192/bjp.177.6.499
85. Bernstein DP, Stein JA, Newcomb MD, et al. Development and validation of a brief screening version of the Childhood Trauma Questionnaire. *Child Abuse Negl*. 2003;27(2):169-190. doi:10.1016/S0145-2134(02)00541-0
86. Elgar FJ, Waschbusch DA, Dadds MR, Sigvaldason N. Development and Validation of a Short Form of the Alabama Parenting Questionnaire. *J Child Fam Stud*. 2007;16(2):243-259. doi:10.1007/s10826-006-9082-5
87. Parker G, Roussos J, Hadzi-Pavlovic D, Mitchell P, Wilhelm K, Austin MP. The development of a refined measure of dysfunctional parenting and assessment of its relevance in patients with affective disorders. *Psychol Med*. 1997;27(5):1193-1203. doi:10.1017/S003329179700545X
88. Hagiwara A, Hori M, Kamagata K, et al. Myelin Measurement: Comparison Between Simultaneous Tissue Relaxometry, Magnetization Transfer Saturation Index, and T1w/T2w Ratio Methods. *Sci Rep*. 2018;8(1):10554. doi:10.1038/s41598-018-28852-6
89. Fischl B. FreeSurfer. *NeuroImage*. 2012;62(2):774-781. doi:10.1016/j.neuroimage.2012.01.021
90. Wagstyl K, Paquola C, Bethlehem R, Huth A. kwagstyl/surface_tools: Initial release of equivolumetric surfaces. Published online September 9, 2018.

doi:10.5281/zenodo.1412054
91. Kim JS, Singh V, Lee JK, et al. Automated 3-D extraction and evaluation of the inner and outer cortical surfaces using a Laplacian map and partial volume effect classification. *NeuroImage*. 2005;27(1):210-221. doi:10.1016/j.neuroimage.2005.03.036
92. Glasser MF, Coalson TS, Robinson EC, et al. A multi-modal parcellation of human cerebral cortex. *Nature*. 2016;536(7615):171-178. doi:10.1038/nature18933
93. Kundu P, Inati SJ, Evans JW, Luh WM, Bandettini PA. Differentiating BOLD and non-BOLD signals in fMRI time series using multi-echo EPI. *NeuroImage*. 2012;60(3):1759-1770. doi:10.1016/j.neuroimage.2011.12.028
94. Kundu P, Brenowitz ND, Voon V, et al. Integrated strategy for improving functional connectivity mapping using multiecho fMRI. *Proc Natl Acad Sci*. 2013;110(40):16187-16192. doi:10.1073/pnas.1301725110
95. Cox RW. AFNI: Software for Analysis and Visualization of Functional Magnetic Resonance Neuroimages. *Comput Biomed Res*. 1996;29(3):162-173. doi:10.1006/cbmr.1996.0014
96. Bullmore E, Fadili J, Maxim V, et al. Wavelets and functional magnetic resonance imaging of the human brain. *NeuroImage*. 2004;23:S234-S249. doi:10.1016/j.neuroimage.2004.07.012
97. Fisher RA. Frequency Distribution of the Values of the Correlation Coefficient in Samples from an Indefinitely Large Population. *Biometrika*. 1915;10(4):507-521. doi:10.2307/2331838
98. Worsley K, Taylor J, Carbonell F, et al. SurfStat: A Matlab toolbox for the statistical analysis of univariate and multivariate surface and volumetric data using linear mixed effects models and random field theory. *NeuroImage*. 2009;47:S102. doi:10.1016/S1053-8119(09)70882-1
99. Barbas H. Cortical structure predicts the pattern of corticocortical connections. *Cereb Cortex*. 1997;7(7):635-646. doi:10.1093/cercor/7.7.635
100. Huntenburg JM, Bazin PL, Goulas A, Tardif CL, Villringer A, Margulies DS. A Systematic Relationship Between Functional Connectivity and Intracortical Myelin in the Human Cerebral Cortex. *Cereb Cortex N Y N 1991*. 2017;27(2):981-997. doi:10.1093/cercor/bhx030
101. Zilles K, Palomero-Gallagher N, Grefkes C, et al. Architectonics of the human cerebral cortex and transmitter receptor fingerprints: reconciling functional neuroanatomy and neurochemistry. *Eur Neuropsychopharmacol*. 2002;12(6):587-599. doi:10.1016/S0924-977X(02)00108-6
102. Mesulam MM. From sensation to cognition. *Brain*. 1998;121(6):1013-1052. doi:10.1093/brain/121.6.1013
103. Dorfschmidt L, Bethlehem RA, Seidlitz J, et al. Sexually divergent development of depression-related brain networks during healthy human adolescence. *Sci Adv*. 2022;8(21):eabm7825. doi:10.1126/sciadv.abm7825
104. Larivière S, Paquola C, Park B yong, et al. The ENIGMA Toolbox: multiscale neural contextualization of multisite neuroimaging datasets. *Nat Methods*. 2021;18(7):698-700. doi:10.1038/s41592-021-01186-4